

Performance Prediction of Solar Thermal Water Pump using Artificial Neural Networks

Rohinikumar Bandaru* , Chandrasekharan Muraleedharan

Department of Mechanical Engineering, NIT Calicut, India, 673601

Abstract

The solar thermal pump can be used for handling water where electrical power is not available and solar energy is in plenty. Performance analysis was carried out on a fabricated laboratory scale set up of unconventional solar thermal water pump in Solar Energy Centre of NIT Calicut. The pump employs a flat plate solar collector for converting the working substance (ethyl ether) into vapour and its pressure is adequate to pump water to a fairly high head. The additional storage tank for vapour and a separate condenser cause greater freedom in the pump's operation leading to improved performance. The performance of solar water pump has been analysed for three different delivery heads 3, 4 and 5 m. The artificial neural network model has been applied successfully to predict the performance of the system at different working conditions. The heating time, efficiency and discharge of the pump have been predicted using three different parameters - solar radiation, ambient temperature and discharge head - by the proposed ANN model based on the feed forward back propagation algorithm. ANN predicted results and estimated values of heating time, efficiency and discharge yield correlation coefficients of 0.99326, 0.99548 and 0.9943, and RMSE values of 0.000126, 0.000087 and 0.000316, respectively.

Keywords: *Solar thermal water pump, Experimental analysis, ANN model*

1. Introduction

Pumps which operate utilizing solar energy are significant in countries where the farming communities are scattered over large and distant areas and where electrical power is not readily available [1]. Most of solar thermal water pumping systems studied in the past few decades have the advantages of being simple, inexpensive, ease of manufacture, easily assembled, maintenance free, reliability and non-mechanical [2]. The solar thermal water pumps generally make use of the fact that the increase in volume of a liquid on vaporization at a given pressure is utilized in displacing the water to a higher elevation and the volume reduction during condensation for suction of water for the next cycle of pumping action [3].

Many investigators have modelled, developed and analysed several types of solar thermal water pumping systems. Solar thermal pumps were developed by Rao *et al.* [4] primarily for lift irrigation in 1976. Kwant *et al.* [5] have also studied the

performance of solar water pump that uses displacement tanks in which there is no direct contact between working fluid and the water to be pumped. Sudhakar *et al.* [6] suggested a modified version to this solar pump. Venkatesh *et al.* [7] added few additional tanks to these systems and developed a new version to these systems. Sumathy *et al.* [8] designed experimental set up with cooling coil in tank for condensing the working fluid and conducted experimental studies [9, 2] on solar thermal water pump with both ethyl ether and pentane as working fluids with separate storage tank for a discharge of 15 litres/cycle at 6 m, 8 m and 10 m delivery heads. Sumathy *et al.* [10] also discussed the importance of effective condensation and design of the condensation coil. Effect of the condensation time and heating time on the performance of solar thermal water pump and change in condensation time as well as cycle time with inclusion of separate condenser at different delivery heads were reported by Wong and Sumathy [11].

Analytical performance evaluation of solar thermal water pumping systems is highly complicated due to involvement of

* Corresponding author.

E-mail: rohinikumar@nitc.ac.in

© 2015 International Association for Sharing Knowledge and Sustainability

DOI: 10.5383/ijtee.15.01.001

too many parameters and their inherent nonlinear and transient nature. Artificial neural network (ANN) modelling simplifies these situations and gives faster results [12]. ANNs are able to learn the key information patterns with in multidimensional information domain. Application of ANN for modelling of energy systems were extensively reviewed by Kalogirou [13] and reported that it is a widely accepted technique for predicting the performance of energy systems using non-linear variables. Steady state performance of the vapour compression liquid chiller was modelled by Bechtler *et al.* [14] using ANN and found that the results were in good agreement experimental values. Mohanraj *et al.* [15,16] carried out the performance prediction and exergy analysis of direct expansion solar assisted heat pump using ANN and reported that the models yield very good statistical performance values like correlation coefficient, RMS and COV values. Deepali *et al.* [17] reported the performance of hybrid photovoltaic thermal double pass air collector under different weather conditions using ANN model. Prediction of energy consumption of a passive solar building [18], and modelling of cascade refrigeration system [19] were also done using ANN with acceptable accuracy. From the brief literature review cited, it is observed that many investigators used ANN effectively for performance assessment of thermal and energy systems.

The present work focuses on an unconventional water pump with ethyl ether as working fluid. The inclusion of separate condenser for condensing the vapour facilitates greater freedom in the pump's operation and thereby improves the performance. An unconventional solar thermal water pump has been designed and fabricated with a collector having an area of 1 m². The performance of the pump is evaluated experimentally at three different discharge heads 3, 4 and 5 m. An attempt is made to evaluate the performance of the system at different working conditions with ANN modelling.

2. Solar Thermal Water Pumping System

2.1. System Description

Figure 1 shows the schematic diagram of the solar thermal water pump fabricated for analysis. The pump operates on the following principle: *thermo-siphon circulation of a low boiling point liquid at isochoric conditions in a flat plate collector undergoes evaporation and rise in pressure. This high pressure vapour exerts the required force to lift water to the desired elevation. Ensuing to this, expansion of the vapour causes subsequent decrease in pressure which provides the suction.* The system consists of a flat-plate solar collector coupled to an insulated tank S both containing ethyl ether, insulated vapour storage tank N, insulated brine tank A, air tank B, well tank C, overhead water storage tank D, condenser, sump and a set of valves between the components. The working fluid suitable to this system is primarily based on its normal boiling point and its miscibility with water. The normal boiling point of ethyl ether is 35 °C. It is slightly miscible with water and is found to be immiscible with brine solution [20].

Each working cycle of the pumping system consists of four processes: Evaporation, pumping, suction and condensation. Initially liquid ethyl ether is charged completely in flat plate collector and separation tank S. The vapour storage tank N is in communication with separation tank S. Liquid ethyl ether absorbs solar radiation in the flat plate collector and undergoes phase change after which it flows to tank S due to thermosiphon circulation. By its inherent nature, saturated vapour flows from

tank S to tank N. Due to the progress of similar events, vapour is accumulated in tank N and its pressure increases. Once the predetermined pressure is attained in tank N, valve 1 is closed and valve 2 is opened. The vapour expands from tank N to tank A, which exerts downward force on the brine solution in A and causes the displacement of brine from tank A to tank B. This displaced brine solution compresses the air in tank B and this compressed air in turn pushes water from vessel C to the overhead tank D. This constitutes the two events, evaporation and pumping.

At the end of pumping, valve 2 is closed and valve 1 is opened. Now, tank N is restocked with ethyl ether vapour from the collection system due to pressure difference between them. Concurrently, valve 3 is opened to cause the discharge of expanded vapour from vessel A to condensing chamber of the condenser. During the discharge of the expanded vapour to condenser the pressure in vessel A decreases, as a result the brine solution in vessel B returns to vessel A. During this period, the pressure of air in vessel B returns to its initial value. As a result, the well water is sucked into vessel C through the one-way valve 5. When vessel C is completely filled with water, the water level in vessel A is restored to its initial condition, ensuring the displacement of expanded vapour from tank A to the condensing chamber. At this point, valve 3 is closed to isolate the condenser. Simultaneously, valve 4 is opened to allow the flow of water from overhead tank D through the condenser to condense the vapour in it. This constitutes the suction and condensation processes. Now, the pumping system is ready for the next cycle of operation.

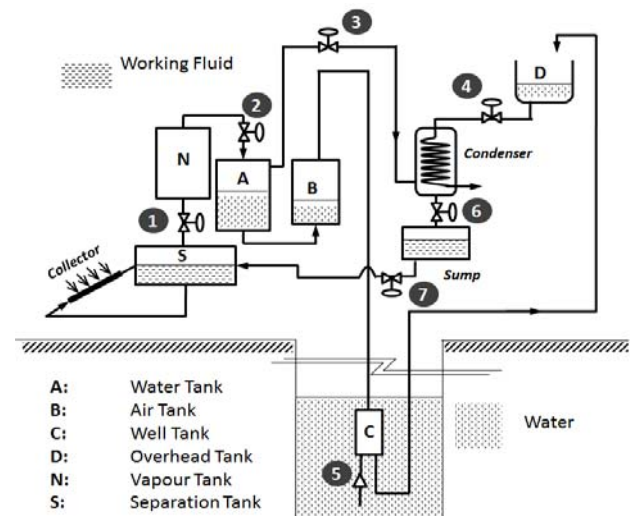


Fig. 1. Schematic diagram of the solar thermal water pump

Inclusion of the separate condenser in the pumping system will improve the performance of the system due to (i) reduction in the condensation time which causes the reduction in the total time required to complete a working cycle, and (ii) saving in time required for the removal of condensed working fluid from tank A after every 5 or 6 working cycles. Figure 2 represents the various states followed by the working fluid during a working cycle on Temperature – Entropy (T-s) coordinates. Process 1-2 represents heating of the working fluid due to thermo-siphon circulation in the collector and separation tank at constant volume. During the process 2-3, the saturated vapour corresponding to pressure at state 2 separated out from tank S and is stored in tank N. Process 3-4 represents isentropic expansion of vapour to the pressure corresponding to discharge head (P_d), in the tanks N and A. At the end of pumping, the

expanded vapour at state 4 in vessel A flows into the condenser to further expansion to reach state 5. The processes 5-6 and 6-7 correspond to the ideal processes of cooling and condensation of the vapour inside the condenser with which the execution of the working cycle will be completed.

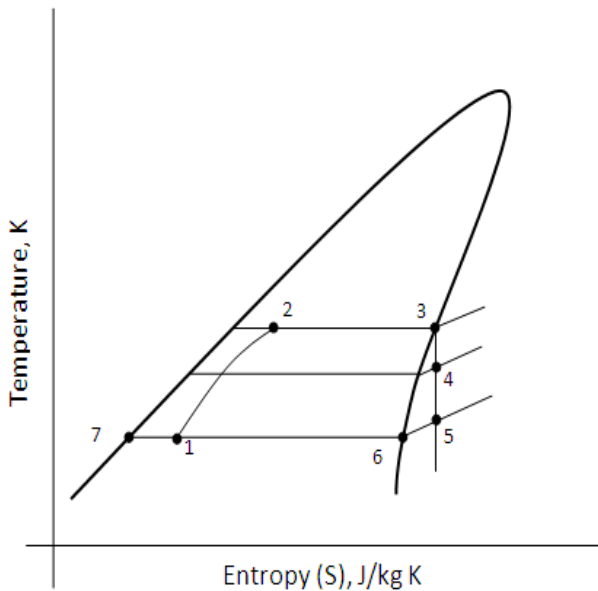


Fig. 2. T-s diagram

2.2. System design

The objective of the system design includes the determination of the volumes of various tanks used in the pumping system, design of the condenser and flat plate collector. The volume of various tanks in the system primarily depends upon the collector area, discharge head of the pump and quantity of water lifted per cycle. This system is designed for a maximum delivery head of 10 m, flat plate collector of exposed area of 1 m² and the quantity of water lifted per cycle 5 litres (i.e. volume of tank C). The optimized volumes of the tanks S, N, A and B are obtained as 12, 15, 15 and 10 litres, respectively. These values are obtained from the detailed consideration of various processes occurring in each of the tanks. The tanks N, S, A and B have a diameter of 300 mm each while tank C has 200 mm diameter. All the tanks have been fabricated in mild steel plate of 3 mm thick.

The condenser used is of shell and coil type, with water from overhead tank D as coil side fluid and expanded ethyl ether vapour from tank A as shell side fluid. The volume of the condensing chamber is obtained by considering the appropriate thermodynamic process for expansion of working fluid from discharge pressure (Pa) in tank A to atmospheric pressure in condensing chamber. The condenser shell (material: mild steel) has a capacity of 30 litres with a diameter of 300 mm. Copper tube of diameter 7 mm having a length of 3 m with 8 turns provides the passage for water in the condenser. The flat plate solar collector, which is the key component in the system, has an exposed area of 1 m². The absorber plate is made of copper sheet of thickness 0.71 mm and is coated with black mat paint to make the solar energy absorption maximum. The collector is well insulated with PUF. The riser tubes and headers are fabricated with copper tube while the outer cover is made of mild steel.

2.3. Experimentation

Figure 3 shows the photograph of the fabricated solar thermal water pump on which experiments were carried out. The experimental set up is located in Solar Energy Centre at National Institute of Technology Calicut, Kerala, India. The solar thermal pumping system was tested under the meteorological conditions of Calicut (latitude of 11.15 °N, longitude of 75.49 °E). Except at C tank, bourdon tube pressure gauges and calibrated J-type thermocouples are provided to measure the pressure and temperature variation at all the components of the system. A digital pyranometer with an accuracy of ± 5 W/m² is placed near the collector to measure the instantaneous solar insolation. The valves used at the required points are manually operated needing frequent inspection during the operation of the pump.

Since the temperature and pressure of vapour are high in the working mode, copper tubes are used to connect the tanks wherever ethyl ether vapour flows in the system. For the handling of brine solution and water PVC pipes are used. Asbestos rope of 10 mm diameter is wound on the surface of the tanks as insulation and a fine coating of plaster of paris is provided over asbestos. Before filling the diethyl ether, system has been evacuated using a high vacuum pump because diethyl ether will form combustible products with air. The charging of the system is done early in the morning to minimize the evaporation of the working fluid. The collector is exposed to the sun at 8.00 AM onwards and it is found that if there is enough radiation, pump is ready for operation by 10.00 - 10.30 AM. Since the pump operation depends on the availability of solar radiation it is found that around noon, pump is having its best performance. Also in the evening when radiation is less, it is not possible to achieve the required pressure.

Experiments were conducted for different heads of 3 m, 4 m, and 5 m and the required data to perform ANN modelling is gathered. It is found that the operating pressures for 3 m, 4 m and 5 m discharge heads are 2 bar, 2.3 bar, and 2.7 bar, respectively. At the end of each day the condensed vapour is stored in the condenser and it is re-circulated in the next day morning for further pumping from sump to S tank.

2.4. Uncertainty Analysis

The errors involved in measuring instruments will influence the accuracy of the calculated results. So, determination of uncertainty in the measurements during experimentation is important. The only measurement required to know performance of the pump is solar radiation and the others such as discharge head and quantity of water lifted per cycle are general observations. The error involved with the pyranometer which is used to measure the solar radiation is ± 5%.

Propagation of uncertainty method [21] can be used to determine the combined effect of random measurement errors. According to this method, the result *R* is a given function of variables *x*₁, *x*₂, *x*₃, *x*₄,.....*x*_{*n*}. Thus,

$$R = R(x_1, x_2, x_3, x_4, \dots, x_n) \tag{1}$$

Let *w_R* be the uncertainty in the result and *w*₁, *w*₂, *w*₃, *w*₄,.....*w*_{*n*} the uncertainties in the independent variables. If the uncertainties in the independent variables are all given with the same odds, then the uncertainty in the result will be,

$$w_R = \sqrt{\left(\frac{\partial R}{\partial x_1} w_1\right)^2 + \left(\frac{\partial R}{\partial x_2} w_2\right)^2 + \left(\frac{\partial R}{\partial x_3} w_3\right)^2 + \dots + \left[\frac{\partial R}{\partial x_n} w_n\right]^2} \tag{2}$$

The uncertainty in the performance parameter (energy efficiency) is found as 0.7245 %.



Fig. 3. Photograph of the solar thermal water pump

3. Artificial Neural Network Development

High processing speeds and short development made the usage of artificial neural network (ANN) an apt tool for forecasting, functional approximation, optimization, simulation, modelling and performance predictions of thermal systems during the past decades [12, 22]. ANNs are composed of simple elements operating in parallel. These elements are inspired by biological nervous systems. They learn the relationship between the input parameters, and the controlled and uncontrolled variables by studying previously recorded data. Another advantage of using ANN is its ability to handle large and complex systems with many inter-related parameters. The network usually consists of an input layer, some hidden layers and an output layer. The number of neurons in the input layer is equal to the number of input parameters and the number of neurons in the output layer is equal to the number of output parameters.

The ANN modelling is carried out in two steps; the first step is to train the network whereas the second is to test the network with data, which are not used for training. Although training takes a long time, they make decisions very fast during operation. ANN is trained with suitable learning method to perform a particular function by adjusting the values of weight coefficient between processing neurons. The training process continues until the network output matches with the desired output. Changing the weights and biases reduces the error between the network output and desired output. The training process is terminated when the error falls below a determined value. The network uses a learning mode, in which an input is presented to the network along with the desired output and the weights are adjusted so that the network attempts to produce the desired output.

The architecture of the network selected with the input and output parameters are shown in Figure 4. The input parameters for this present work are solar radiation received per unit area, delivery head and the ambient temperature. Solar radiation is the radiation falling on the collector for the corresponding heating time in a specific cycle. The second input parameter is the delivery head of pump and the present work is carried out for three delivery heads 3 m, 4 m and 5 m. Third input parameter, ambient temperature is also noted down for each heating time value. The output parameters in this work are heating time for each cycle of pumping, efficiency of the pump and the discharge from the system. Heating time is the time needed to build up the required pressure in N tank for the next cycle of pumping after the completion of each cycle. Every morning, pressure will be low so the heating time for the first cycle will be always higher. After the first cycle, pressure of vapour in tank N will not be very low. So, for the subsequent cycles, pressure of vapour in tank N builds up from a value and the heating time will be less. Efficiency is the ratio of hydraulic work done for a particular delivery head in a pumping cycle to the solar energy input to that cycle. Mathematically,

$$\eta = \frac{\rho_w V_w g H}{I_\beta} \tag{3}$$

Where H is discharge head in m, V_w is volume of water lifted and I_β is solar radiation intensity in W/m^2 .

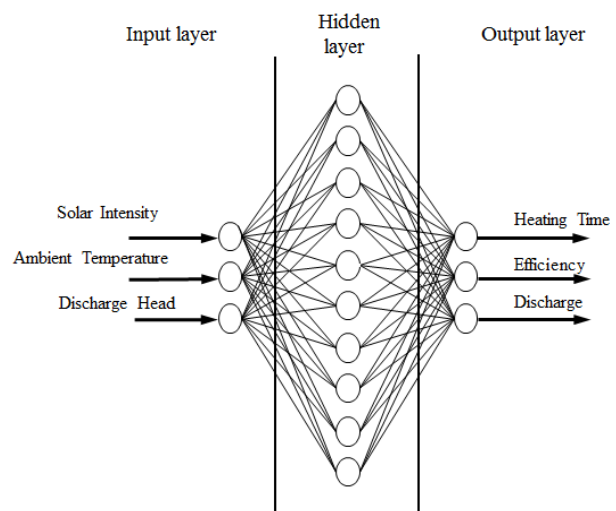


Fig. 4. Network architecture for the pumping system

The experimental data obtained is used to train the network. Here 90 data sets are used to train the network. The input data are divided into training sets (70%), validation sets (15%) and testing sets (15%). In this modelling, the learning algorithm used is “Feed forward Back propagation” with single hidden layer network. This algorithm optimizes the synaptic weight by allowing the error to spread from output layers towards the lower layers (hidden layer and input layer). The output of the network is compared with desired output at each epoch and errors are computed. These errors are then back propagated to the ANN for adjusting the weights such that the errors decrease with each iteration and ANN model approximates the desired output. The network is trained till the chosen error goal is achieved.

Here in this work Tan sigmoid transfer function is used as the activation function for both the hidden layer and the output layer. The general form of the Tan sigmoid function [23] is,

$$\sigma(t) = \frac{e^t - e^{-t}}{e^t + e^{-t}} \quad (4)$$

where, t is the weighted sum of inputs.

The values of the training and test data are normalized to a range of 0–1 for easy converge. Training function used was Levenberg-Marquardt function with input layer consisting of three neurons and output layer having three neurons. The number of neurons in the hidden layer is chosen based on the correlation coefficient. From Table 1 it is clear that when the number of neurons in the hidden layer is 10, Correlation coefficient has its highest value.

Table1. Correlation coefficient for different number of neurons

No of neurons in hidden layer	Correlation coefficient
6	0.99588
8	0.99774
10	0.99915
12	0.99629
14	0.9971

Learning is based on gradient descent (LEARNGDM) where minimum gradient is set as 1e-008. Performance function adopted is mean square error (MSE). The performance of the ANN model is evaluated in terms of three statistical parameters. They are coefficient of correlation (CC), average percentage error (APE) and root mean square error (RMSE). These are computed according to the following equations [23].

$$RMSE = \sqrt{\frac{\sum (X_i - Y_i)^2}{N}} \quad (5)$$

$$CC = \frac{N \sum (X_i Y_i) - \sum X_i \sum Y_i}{\sqrt{(N \sum X_i^2 - (\sum X_i)^2)(N \sum Y_i^2 - (\sum Y_i)^2)}} \quad (6)$$

$$APE = \frac{1}{N} \sum \left(\frac{abs(X_i - Y_i)}{X_i} \right) \times 100 \quad (7)$$

Where X_i = the experimental values and Y_i = the ANN predicted output values

4. Results and Discussion

The experiments were conducted for three different delivery heads of 3 m, 4 m and 5 m. The availability of solar radiation is maximum at a place like Calicut during this period. The maximum solar radiation during the test period was found to be around 900 W/m². The experiments were conducted continuously for one week at each delivery head. Every day the collector was exposed to radiation from 8.00 AM onwards and the pump was ready to execute its first cycle by 10.30 AM. Consistent results at each discharge head were observed on all days at a particular discharge head.

The variation of the solar radiation with time on a typical solar day in which the experiments were conducted is plotted in Figure 5. The solar radiation is very less in the morning and gradually increases till the noon thereafter it decreases which is a standard trend of variation. But the maximum availability of solar radiation in a day compatible to the experiment is found to be between 10.30 AM and 3.00 PM. The pump is expected to give the best performance during this time interval and the experimental results are exactly matching. The heating time at noon time is found to be much lesser as compared to other time. The ambient temperature variation (Figure 6) also shows the same trend of the solar radiation curve as the solar radiation directly influences the ambient temperature.

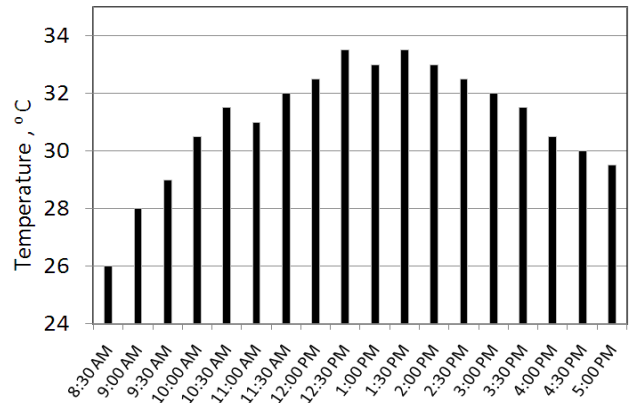


Fig. 5 Variation of solar radiation with time

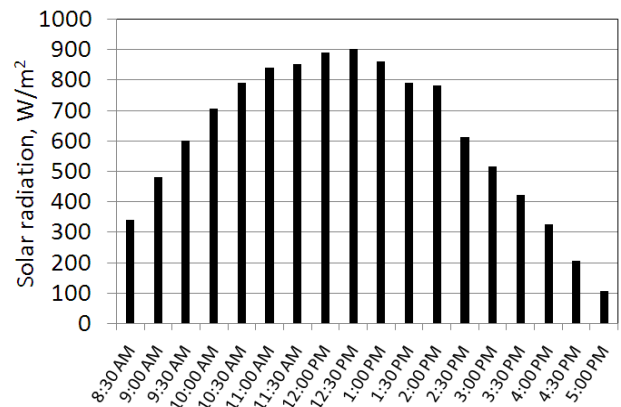


Fig. 6 Variation of ambient temperature with time

When the pump is in operation, once the required pressure in tank N reaches, the valve 2 is opened and valve 1 is closed, the vapour expands to push the brine solution from tank A to tank B to achieve pumping. During this period, S tank is isolated from N tank so the pressure in N tank only is reduced. Once pumping is over, valve 2 is closed and valve 1 is opened. When tank N is in communication with tank S (after the expansion from tank N to tank A and the opening of valve 1) there will be a flashing of high pressure vapour from S tank to N tank to reach the equilibrium state between the two tanks. This flashing of vapour reduces the pressure in the S tank to a lower value and equilibrium pressure is attained between these two tanks. For a head of 3 m it is found that the pressure reduces from the discharge pressure of 2 bar to 1.34 bar. The pressure again has to reach at least the minimum value for the next cycle to perform. The time taken for this is called as the heating time. Figure 7 shows the exact variation of the pressure when the pump is in

operation at 3 m delivery head which has the nature of fluctuating between two limits.

Table 2 shows the effect of delivery head on the number of cycles performed per day for the pump. It is found that the maximum number of cycles that the pump performed for a head

of 3 m is 7 and as expected it is getting reduced to 4 times for a head of 4 m and 3 times for 5 m head. The reason for the reduction in number of cycles is as head increases the pressure required for pumping increases and more time is needed to achieve the required pressure.

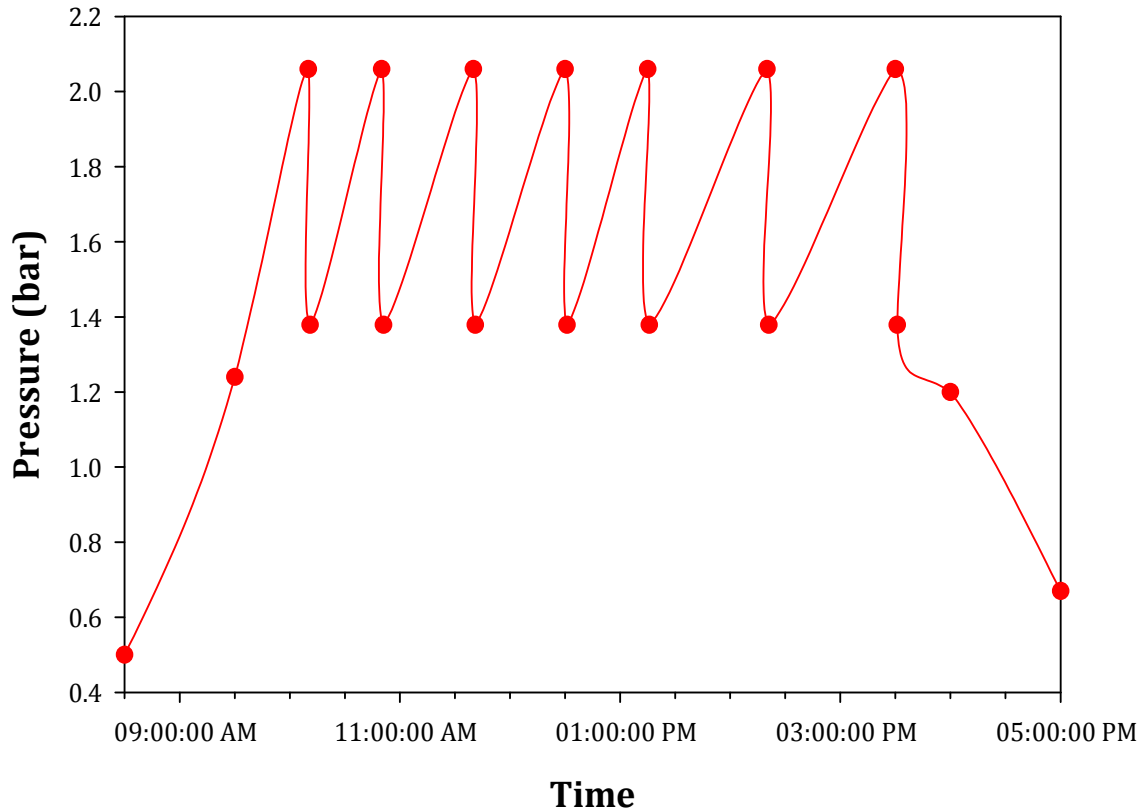


Fig. 7 Pressure variation in S tank when pump is in operation

The maximum quantity of water pumped in a day is found to be 35 litres for a head of 3 m and the same at a head of 5 m is found to be 15 litres as shown in Table 2. Efficiency depends upon the number of cycles per day and the work output per cycle at a discharge head. Since the effect of increase in efficiency due to increase in work output per cycle dominated by the effect of decrease in efficiency due to reduction in number of cycles per day at higher delivery heads, efficiency decreases with increase in delivery head.

It is clear from the performance analysis that as the head increases heating time also gets increased since required pressure for pumping is more. Since the performance parameters like efficiency and discharge of water are depending on heating time, they are also getting reduced as the head increases. There is little difference in the theoretical pressure calculated to pump water and the actual pressure. This may be due to the condensation of some amount of vapour while coming in contact with the brine solution in tank A. This condensation reduces the pressure inside the tank. It is found that the difference in theoretical and actual pressure is getting increasing as head increases. The more the difference in temperature between brine solution and vapour, more will be the rate of condensation. During the experiment it is noticed that some amount of vapour is reaching even up to C tank.

Table 2. Number of cycles per day, discharge and efficiency

S. No.	Delivery Head (m)	No. of cycles per day	Discharge (litres/day)	Efficiency $\times 10^{-2}$ %
1	3	7	35	0.14
2	4	4	20	0.125
3	5	3	15	0.09

ANN modelling is carried out using the 90 sets of experimental readings gathered. From the test data, heating time, efficiency of the pump and discharge are simulated for different discharge heads of 3 m, 4 m and 5 m using the model developed by the ANN. Experimental results are compared with ANN predictions for heating time, efficiency of the cycle and discharge at three different discharge heads against solar radiation and ambient temperatures in the form nine subplots in Figure 8. The results confirm that the ANN predicted values are in good agreement with the experimental values.

The performance of the ANN model is evaluated in terms of three statistical parameters- coefficient of correlation (CC), average percentage error (APE) and root mean square error (RMSE). The comparison between the ANN predictions and estimated values of heating time, cycle efficiency and discharge yields correlation coefficients of 0.99326, 0.99548 and 0.99430, respectively. The RMS and APE values for heating time, cycle efficiency and discharge are shown in Table 3.

Table 3. Performance parameters for ANN model

Parameters	Heating time	Efficiency	Discharge
RMSE	0.000126	0.000087	0.000316
CC	0.99326	0.99548	0.99430
APE (%)	2.82	2.58	3.95

5. Conclusions

Experiments on fabricated solar thermal water pump have been carried out for different delivery heads of 3 m, 4 m and 5 m. The performance parameters - heating time, efficiency of the pump and discharge - were estimated. The pump is found to be capable of operating 7 cycles per day. The heating time for the working fluid and condensation of the vapour are found to be the critical factors for time required to complete any working cycle. The high heating time for every working cycle at any delivery head was observed as a significant reason for obtaining less number of cycles per day which can be improved by using a more efficient solar collector. Since the number of cycles per day is less the overall efficiency of the pump obtained ($0.14 \times 10^{-2} \%$) is also very less than expected. Artificial neural network model is developed to evaluate the performance of the pumping system at different working conditions. ANN predicted results and estimated values of heating time, efficiency and discharge yield correlation coefficients of 0.99326, 0.99548 and 0.9943, and RMS values of 0.000126, 0.000087 and 0.000316, respectively.

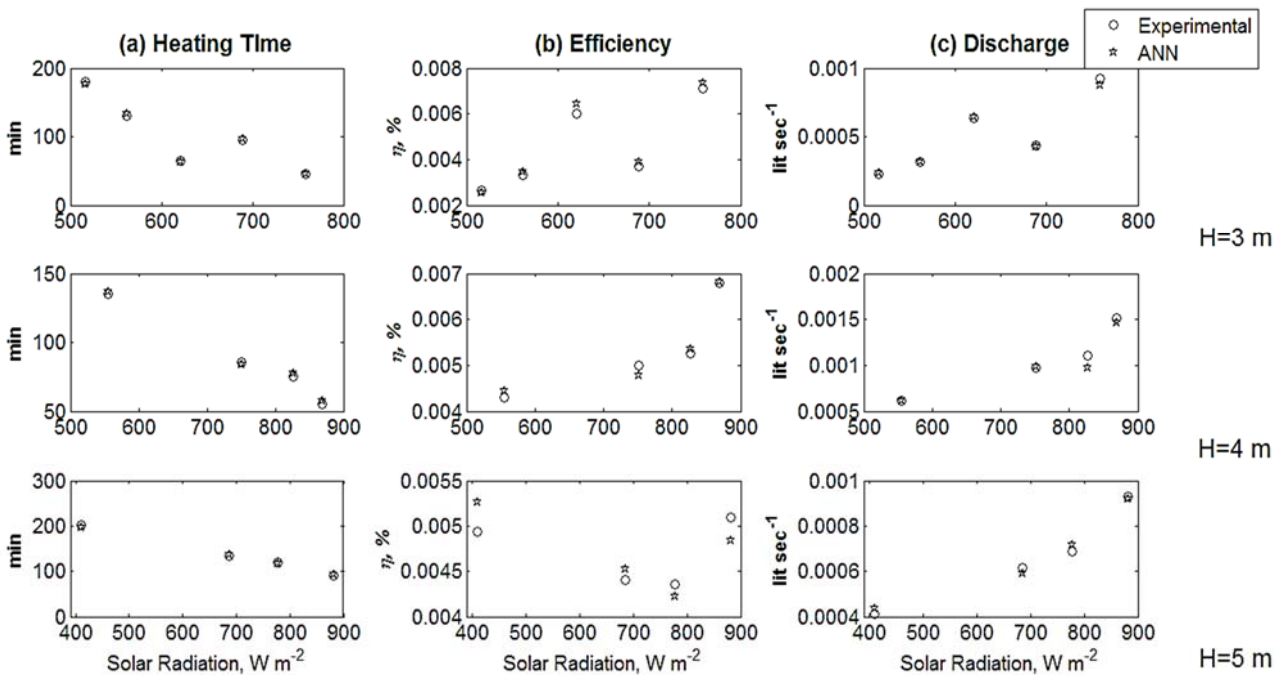


Fig. 8. Comparison of experimental and ANN predictions of (a) heating time, (b) efficiency and (c) Discharge with respect to solar radiation for three discharge heads (H=3,4 and 5 m)

References

- [1] Muralidhar. H.P. A review of solar pumps and their principles. Proceedings of the International Solar Energy Society Congress, New Delhi, India, 1978, pp. 21- 29.
- [2] Wong. Y.W, Sumathy. K. Performance of solar water pump with ethyl ether as working fluid. Renewable Energy, 2001, vol. 22, pp. 389-394.
- [3] Wong. Y.W, Sumathy. K. Performance of solar water pump with n-pentane and ethyl ether as working fluids. Energy Conversion and Management, 2000, vol. 41, pp. 915-927.
- [4] Rao. D.P, Rao. K.S. Solar water pump for lift irrigation. Solar Energy, 1976, vol. 18, pp. 405-411.
- [5] Kwant. K.W, Rao. D.P, Srivstava. A.K. Experimental studies of a solar water pump. Proceedings of the International Solar Energy Society Congress, New Delhi, India, 1978, pp. 1917-21.
- [6] Sudhakar. K, Muralikrishna. M, Rao. D.P, Soin. R.S. Analysis and simulation of a solar water pump for lift irrigation. Solar Energy, 1980, vol. 24, pp. 71-82.
- [7] Venkatesh. A. Solar thermal water pump. Proceedings of the International Solar Energy Society Congress, Denver, Colorado, USA, 1991, pp. 2135-40.

- [8] Sumathy. K. Experimental studies on solar thermal water pump. *Applied Thermal Engineering*, 1999, vol. 19, pp. 449-459.
- [9] Sumathy. K, Venkatesh A, V. Sriramulu. A Solar thermal water pump. *Applied Energy*, 1996, vol. 53, pp.235-243.
- [10] Sumathy K, Venkatesh A, Sriramulu V. The importance of the condenser in a solar water pump. *Energy Conversion and Management* ,1995, vol. 36, no.12, pp. 1167-1173.
- [11] Wong. Y.W, Sumathy. K. Thermodynamic analysis and optimization of a solar thermal water pump. *Applied Thermal Engineering*, 2001, vol.21, pp. 613-627.
- [12] Sivanandam. S.A, Sumathi. S, Deepa. S.N. Introduction to neural Network using MATLAB 6.0. 1st ed, Tata McGraw-Hill Publishing Company Limited; 2006.
- [13] Kalogirou SA, Applications of artificial neural-networks for energy systems. *Applied Energy*, 2000, vol 67, pp. 17-35.
- [14] Bechtler. H, Browne .M. W, Bansal. P. K, Kecman. V. New approach to dynamic modelling of vapour-compression liquid chillers: Artificial Neural Networks. *Applied Thermal Engineering*, 2001, vol. 21, pp. 941-953.
- [15] Mohanraj. M, Jayaraj. S, Muraleedharan. C. Exergy analysis of direct expansion solar-assisted heat pumps using artificial neural networks. *International Journal of Energy Research*, 2009, vol. 33, no. 11, pp. 1005-1020.
- [16] Mohanraj. M, Jayaraj. S, Muraleedharan. C. Performance prediction of Direct expansion Solar assisted heat pump using artificial neural networks. *Applied Energy*, 2009, vol. 86, no. 11, pp. 1442-1449.
- [17] Deepali Kamthania, Tiwari. G.N. Performance analysis of a hybrid photovoltaic thermal double pass air collector using ANN. *Applied Solar Energy*, 2012, vol. 48, no. 3, pp. 186-192.
- [18] Kalogirou. S.A, Bojic. M (2000). Artificial neural networks for the prediction of energy consumption on a passive solar building. *Energy*, 2000, vol. 25, no. 5, pp. 479-491.
- [19] Hosoz. M, Ertunc. H.M. Modelling of cascade refrigeration system using artificial neural networks. *International Journal of Energy Research*, 2006, vol. 30, pp. 1200-1215.
- [20] Xie.W.H,Shiu.W.Y, Mackay. D. A review of the effect of salts on the solubility of organic compounds in seawater. *Marine Environmental Research*, 1997, vol. 44, pp. 429-44.
- [21] Beckwith, Marangoni, Leinhard. *Mechanical measurements*. 2004, Pearson Education.
- [22] Priddy. K. L, Keller. P. E. *Artificial Neural Networks*. Prentice-Hall, 2005, Eastern Economy Edition.
- [23] Yilmaz Yoru, T.H.Karakok, Arif Hepbasli. Application of Artificial Neural Network method to exergy analysis of thermal systems. *Fourth International conference on machine learning and applications*, 2009, pp. 715-718.